Formulation of a 3D fully coupled thermo-mechanical finite element model for simulating orthogonal cutting of Ti-6Al-4V

Munoz, Raul; Soo, Sein; Aspinwall, David

Citation for published version (Harvard):
Munoz, R, Soo, S & Aspinwall, D 2013, Formulation of a 3D fully coupled thermo-mechanical finite element model for simulating orthogonal cutting of Ti-6Al-4V. in G Byrne, B Mullany, P Connolly, E Ahearne & N Green (eds), Proceedings of the 30th International Manufacturing Conference : IMC 30. University College Dublin Press, pp. 84-93, International Manufacturing Conference, 30th (IMC30), Dublin, Ireland, 3/09/13.

FORMULATION OF A 3D FULLY COUPLED THERMO-MECHANICAL FINITE ELEMENT MODEL FOR SIMULATING ORTHOGONAL CUTTING OF TI-6AL-4V

R.E. Munoz[1], S.L. Soo[1] and D.K. Aspinwall[1]

1. Machining Research Group, School of Mechanical Engineering, University of Birmingham, Edgbaston, Birmingham, UK.

ABSTRACT

The present investigation involved the formulation of a 3D fully coupled thermo-mechanical finite element model for the orthogonal cutting of Ti-6Al-4V alloy using the general purpose, commercial software ABAQUS. The workpiece material was assumed to follow the Johnson-Cook constitutive relationship while the Cockcroft-Latham damage criterion was implemented into the program via the development of a VUMAT user subroutine in order to simulate chip formation/morphology. Similarly, the cutting tool was defined as a deformable body based on the mechanical/physical properties of ISO K20 tungsten carbide. Predicted response measures such as cutting forces were compared and validated against experimental data for cutting speeds of 60, 90 and 120m/min and a fixed feed of 0.125mm/rev. Simulated cutting forces showed good agreement with corresponding experimental results (3-15% error) while predicted process temperatures agreed well with results published by other researchers. Modelled serrated chip morphology was validated by micrographs of etched chip cross sections, which suggested that the VUMAT user subroutine employed was appropriate.

KEYWORDS: machining, finite element modelling, titanium

1. INTRODUCTION

Finite element (FE) modelling of the machining process has been employed since the 1970's [1] to predict parameters such as temperatures and stresses generated at the tool-chip interface. Computational considerations meant that much of the work undertaken centred on 2D orthogonal turning under plane strain conditions, with more recent work addressing 3D formulations. The range of workpiece materials that has been evaluated is fairly broad and includes alloy steels [2], stainless steels [3], titanium alloys such as Ti-6Al-4V [4] and nickel based superalloys such as Inconel 718 [5]. In particular, FE simulation of Ti-6Al-4V machining represents a significant challenge, not least because of its complex microstructure and enhanced mechanical properties [6]. While the range of titanium alloys is extremely diverse, Ti-6Al-4V ($\alpha+\beta$ alloy) is the most common variant used in industry, accounting for ~ 50% of titanium tonnage worldwide.

Modelling the chip morphology of Ti-6Al-4V represents a considerable task. Previously used Eulerian formulations to model this material had limitations due to the need to predefine a constant deformed chip shape. More appropriate techniques have involved Lagrangian based configurations incorporating a damage model or Arbitrary Lagrangian Eulerian (ALE) approaches with adaptive remeshing (with the option of including a damage model). In both cases, the chip forms freely and its shape is obtained according to the calculations carried out by the FE software. The ALE method usually relies on lengthy iterations to establish refined remeshing parameters, which are time consuming as they are obtained by trial and error. Alternatively, the application of damage models to trigger material failure is a more direct method, and consequently the Johnson-Cook (JC) fracture criteria [7] has been the preferred choice by many researchers.

Chip serration modelling involves two mechanisms namely adiabatic shear and fracture. The incorporation of the former obviously does not require a damage model as any chip serration is caused by localised softening in the workpiece shear zone. Calamaz et al. [8] and Karpat [9] used the ALE technique together with modified material constitutive models to account for the thermal softening produced in the primary deformation region of Ti-6Al-4V resulting in good correlation between their predictions and experiments. However, the drawback of modified material models is that they fit the experimental results without considering any metallurgical/physical attributes of the material. Early work undertaken by Ng [10] on the use of Lagrangian formulations for simulating orthogonal cutting of hardened steel proved successful, however, the author appears to have made use of an ‘artificial separation layer’ to model chip formation and also created pre-formed cracks in selected areas of the workpiece to reflect serrated chips. Similarly Chen et al. [11] working on Ti-6Al-4V, used the JC damage model and an energy-based fracture relationship to simulate onset of damage and chip morphology evolution respectively. An additional (shear) damage criterion to account for chip formation was also utilised. Their modelling strategy was aimed at cutting velocities and feeds up to 4800m/min and 70μm/rev respectively and under such machining conditions, they found that the onset of damage and chip morphology were accurately predicted. However, the damage criterion used for chip formation was also applied to an artificial separation layer.

A different approach was adopted by Shivpuri et al. [12] who employed the Cockcroft-Latham (CL) damage model [13] to simulate the turning of Ti-6Al-4V at a depth of cut of 2.54mm for cutting velocities of 60, 120 and 240m/min together with feeds of 0.127 and 0.35mm/rev. Understandably, it was found that the crack responsible for triggering damage occurred in the region associated with maximum principal and shear stresses. Umbrello [14] investigated several sets of constants for the JC plasticity model [15] in conjunction with the CL damage model when simulating the orthogonal cutting of Ti-6Al-4V alloy. The study focused on cutting speeds of 60, 120, 1200 and 4800m/min to test the accuracy of both constitutive and damage models when predicting cutting forces and chip morphology. The FE predictions showed good correlation with experiments and supported the fact that the CL damage model was not only able to predict serrated chips, but also their geometrical characteristics (chip pitch, peak and valley) with an acceptable level of accuracy.

The present paper details the development of a 3D fully coupled thermo-mechanical FE model to simulate the orthogonal cutting of Ti-6Al-4V alloy using ABAQUS. The constitutive response of the material was described according to the JC plasticity relationship while chip formation/morphology was realised using the CL damage model. Unlike previously published work, no adaptive remeshing schemes or artificial workpiece separation layers were employed, and the damage model was applied to all workpiece elements.

2. EXPERIMENTAL SETUP

The workpiece material was a 105mm diameter bar of Ti-6Al-4V ($\alpha+\beta$ alloy) in the annealed condition. A face grooving operation was performed to produce a 1mm thick tube section in order to simulate orthogonal cutting conditions. All trials were carried out on a Dean Smith & Grace 1910 manual lathe involving tungsten carbide inserts designated as TCMW 16T308 H13A. The corresponding toolholder (STGCR 2525M 16) provided rake and clearance angles of 0° and 7° respectively. Three different cutting speeds of 60, 90 and 120m/min were utilised at a constant feed of 0.125mm/rev.

Cutting forces were measured using a Kistler 9263 three-component piezoelectric dynamometer connected to a series of model 5011 charge amplifiers via suitable coaxial cables. The data from the dynamometer were acquired using a Keithley DAS1601 analogue/digital board and processed with Dynoware software. Measurements were recorded within the first 10-20 seconds of machining, depending on the cutting speed employed. Figure 1 shows the experimental setup used together with the equivalent meshed FE model.

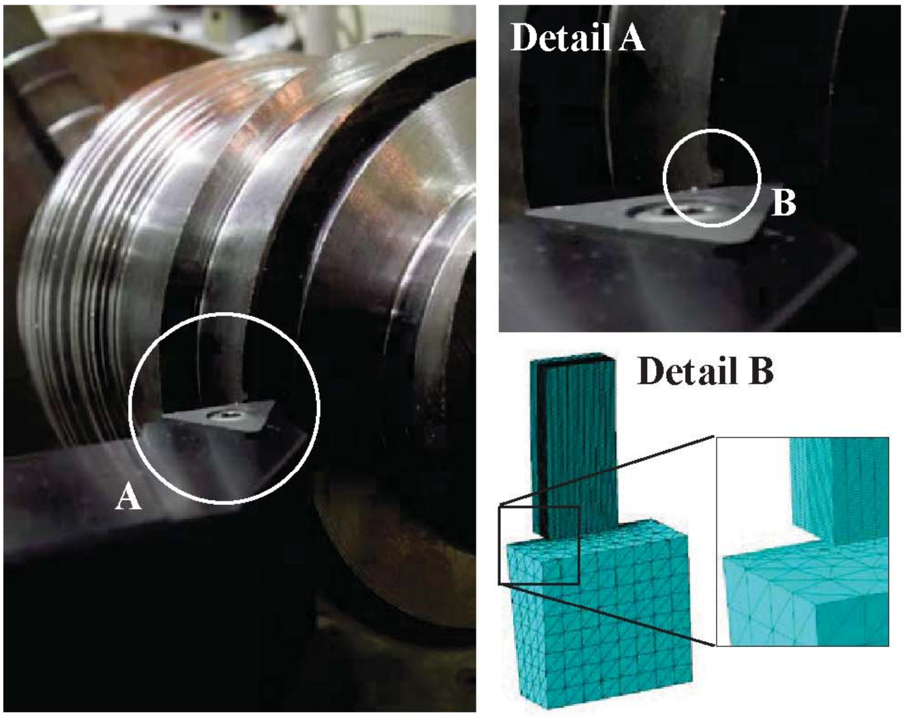

Figure 1: Experimental setup and corresponding meshed FE model

3. FORMULATION OF THE 3D FE MODEL

3.1 Model configuration

The model geometry was developed using the commercial FE pre-processor ABAQUS/CAE 6.10-1, while numerical simulations were performed with the ABAQUS/Explicit module. For simplicity, the tool cutting edge was assumed to be sharp while operating conditions/parameters were defined to match that employed in the orthogonal turning trials. In all the models, the tool and workpiece were meshed with C3D8R linear hexahedral type elements with hourglass control and C3D4 linear tetrahedral type elements utilising distortion control respectively. Although there were minor differences between each simulation, the workpiece and cutting tool were meshed with approximately 43,750 and 4,850 elements respectively. An appropriate uniform mass scaling value was utilised in order to speed up the calculations, without unduly influencing the numerical results [16]. All analyses were carried out on an Intel Xeon CPU with 20 GB of RAM, each run taking ~ 110h of computation.

3.2 Constitutive material and damage models

The Ti-6Al-4V workpiece material was described according to the JC plasticity model [15], where the flow stress is a function of strain (ε), strain rate ($\dot{\varepsilon}$) and temperature (T) as shown in Equation (1);

$$\sigma = [A + B(\varepsilon^n)]\left[1 + C\ln\left(\frac{\dot{\varepsilon}}{\dot{\varepsilon}_0}\right)\right]\left[1 - \left(\frac{T - T_r}{T_m - T_r}\right)^m\right] \quad \text{--------------------------------- (1)}$$

where A=724.7MPa, B=683.1MPa, C=0.035, n=0.47 and m=1, $\dot{\varepsilon}_0 = 10^{-5}$ 1/s is the normalisation strain rate and T_m=1873K and T_r=293K are the melting and reference temperatures respectively [17]. It was also assumed that 90% of the plastic work was converted to heat.

The CL damage model was utilised in all simulations where the work done per unit volume was the main criterion when describing failure of materials, with the maximum principal stress responsible for triggering workpiece damage (achieved via element deletion). This can be quantitatively described as detailed in Equation (2);

$$C = \int_0^{\bar{\varepsilon}_f} \sigma_1 \, d\bar{\varepsilon}^{pl} \quad \text{--- (2)}$$

where C is a material constant, σ_1 is the maximum principal stress and $\bar{\varepsilon}_f$ is the plastic strain at failure. In line with previous work [18], only positive values of σ_1 were considered, hence $\sigma_1 = \sigma_1, \sigma_1 > 0$ and $\sigma_1 = 0, \sigma_1 \leq 0$. The CL damage model was incorporated into the FE model through a VUMAT user subroutine. Additionally, the JC model was developed within the code as the constitutive response of the material was mandatory to calculate the maximum principal stress. Although ABAQUS offers the built-in utility routine 'vsprinc' to obtain principal stress values, a bespoke subroutine to perform this function was embedded in the primary VUMAT, as the former demonstrated considerable numerical instability during the initial time increments. After a series of trial and error iterations, the parameter C was set to 180J/m^3. The VUMAT subroutine was coded using FORTRAN 77 programming language and subsequently compiled and linked to ABAQUS using Intel Visual FORTRAN 10.1 and Microsoft Visual Studio 2008 software solutions.

3.3 Frictional and thermal effects

It is generally accepted that two frictional regions are created at the tool-chip interface during cutting, namely sliding and sticking zones. As it is difficult to calculate the lengths of these zones analytically, one option is to specify them by defining a limiting shear stress [19]. In this study, the restrictions associated with ABAQUS were such that contact at the tool-chip interaction was defined according to the Coulomb friction model with an average friction coefficient (μ) of 0.57, which was calculated based on information from the literature [9, 14].

Apart from the properties of specific heat capacity and thermal conductivity, the thermal contact conductance (TCC) or heat transfer coefficient between the tool and workpiece was also a required input parameter. The TCC essentially determines the temperature drop between two (ideally flat) surfaces in contact and is very sensitive to their mechanical state (e.g. surface roughness) [20]. A high value of TCC can be beneficial as the thermal conductance resistance (1/TCC) would be sufficiently small to guarantee temperature continuity between the bodies in contact. In metal cutting operations, the tool-chip interaction is extremely complex and there is currently no definitive method for determining the TCC. However, a mean TCC value of 100kW/m^2°C was adopted in the present work based on appropriate information in the literature [21]. Table 1 summarises the material [9, 11], contact and thermal properties [9] of the Ti-6Al-4V and cutting tool [22] material (some of which varied with temperature) used in the FE simulations.

Table 1: Various mechanical and thermal property data for Ti-6Al-4V and the carbide cutting tool (temperature in Kelvin)

		Ti-6Al-4V	Tool
Material	Density [kg/m^3]	4430	15000
	Poisson's ratio [-]	0.34	0.22
	Modulus of elasticity [GPa]	111.672-0.0577(T-273)	630
Contact	Heat partition coefficient [-]	0.5	
	Friction coefficient [-]	0.57	
	Plastic work converted to heat [%]	90	
Thermal	Specific heat capacity [J/kgK]	$609.481e^{(0.0002T)}$	402
	Thermal conductivity [W/mK]	0.015T+7.7	100
	Coefficient of thermal expansion [10^{-6}/K]	7+0.003T	-
	TCC [kW/m^{2}K]	100	

4. RESULTS AND DISCUSSION

4.1 Cutting force prediction

Table 2 shows the experimental and predicted tangential and thrust forces for the different cutting conditions employed. Although the FE simulated forces were overestimated in all cases, the maximum discrepancy was less than 15%, suggesting that the assumptions made when developing the 3D FE model were acceptable/reasonable. Figure 2 displays the Von Mises stress distribution in the tool for the first ~ 0.15ms of cutting. As expected, the stresses increased as machining progressed until a sharp drop of approximately 10-15% was recorded corresponding to initiation of the saw-tooth chip profile. This response was repeated continuously with the stresses oscillating between the maximum and minimum values over the entire process duration in line with the experimental force data.

Table 2: Comparison between experimental and predicted average forces

Feed, f [mm/rev]	0.125		
Cutting speed, v [m/min]	**60**	**90**	**120**
Exp. tangential force [N]	143	138	132
ABAQUS prediction [N]	161 (13%)	152 (10%)	149 (13%)
Exp. thrust force [N]	55	52	48
ABAQUS prediction [N]	58.3 (6%)	50.6 (3%)	51 (6%)

Note: Values in brackets show percentage (%) discrepancy from experimental data

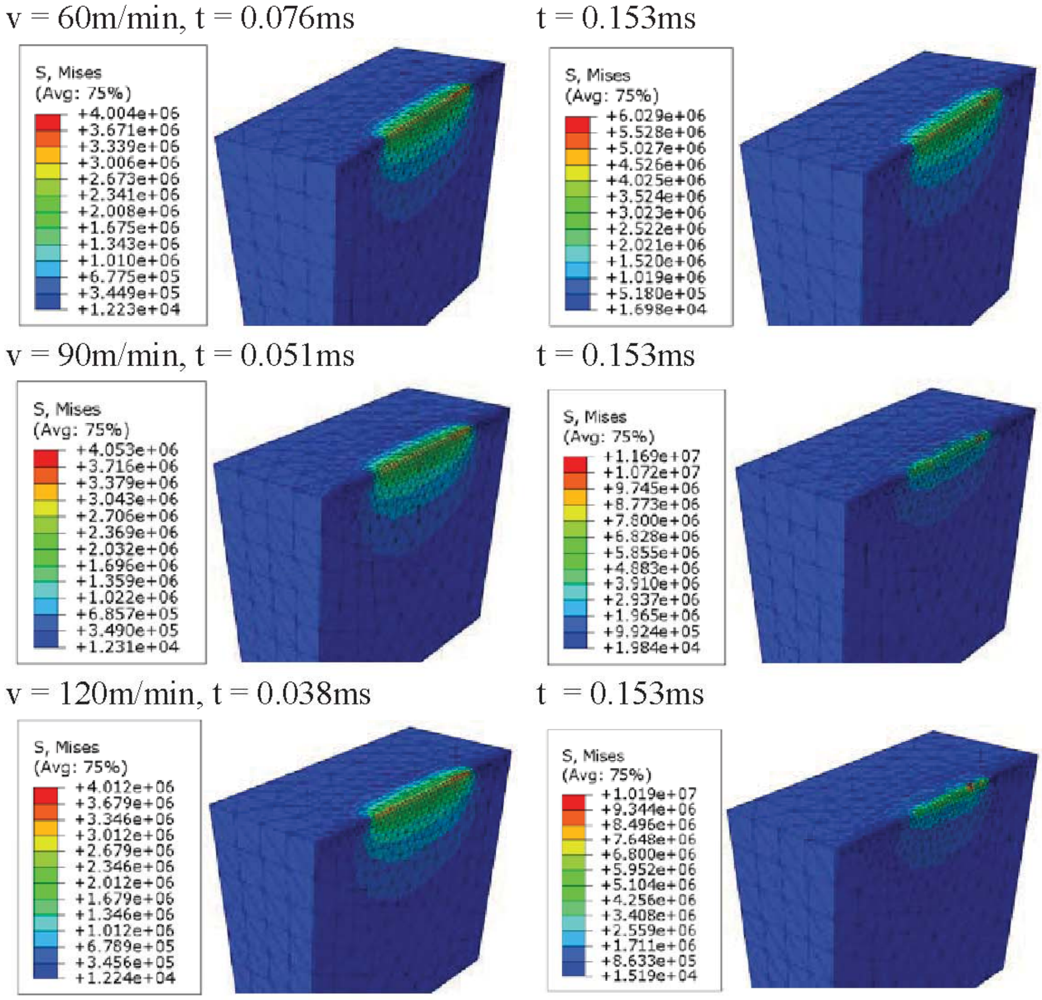

Figure 2: Predicted Von Mises stress distribution in tool [10^{-3}MPa]

4.2 Chip formation/morphology prediction

Figure 3 shows the predicted chip morphology as well as the modulus of elasticity distribution from the FE models together with corresponding cross sectional micrographs of chips collected following the experimental trials. Serrated chip formation was simulated irrespective of cutting speed, which reflected the morphology of swarf detailed in the optical micrographs. However unlike the experimental results, the predicted chips were also discontinuous with premature separation of the segments along the shear bands. This suggests that the damage model employed or failure criterion specified requires further refinement in order to improve the accuracy of the simulation.

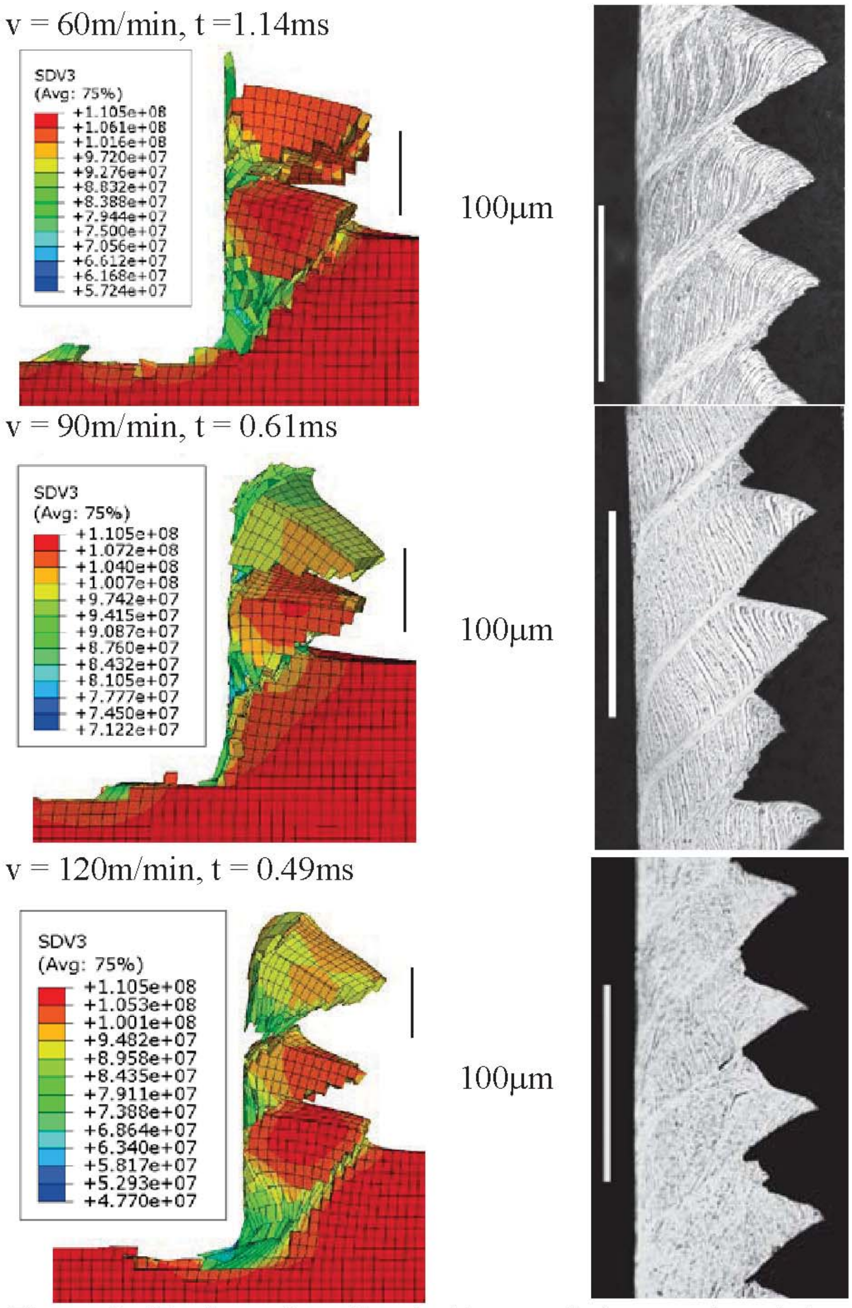

Figure 3: 2D view of predicted chip morphology and modulus of elasticity distribution [10^{-6}GPa]

4.3 Tool and workpiece temperature prediction

Figure 4 displays the predicted temperature distribution in both the tool and workpiece/chip for the different cutting speeds evaluated. Tool-chip contact length generally decreased as cutting speed was increased, with corresponding maximum rake face temperatures of up to 450K when turning at 120m/min. This was typically concentrated along the cutting edge (maximum depth of cut position) with a ‘parabola-like’ temperature distribution pattern extending to the point where the chip loses contact with the tool.

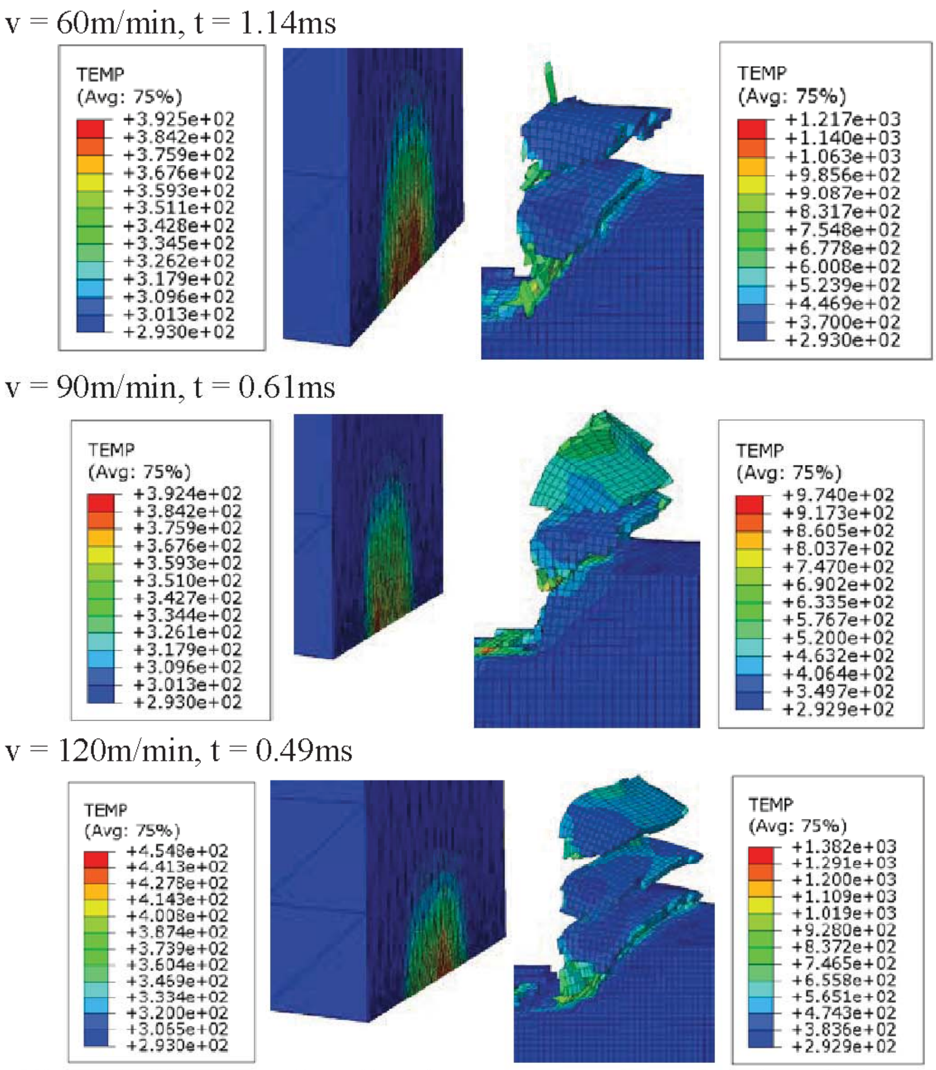

Figure 4: 3D view of predicted temperatures in tool and workpiece [K]

The highest temperatures in the workpiece were recorded along the secondary shear zone due to frictional interactions between the chip and cutting tool surface. This was predicted to exceed ~ 1300K when operating at 120m/min, which was approximately in line with results reported by Sima and Ozel [4]. This confirms that the majority of heat generated remains confined in the chip with greater dissipation of thermal energy through the cutting tool as a result of the higher thermal conductivity in the latter. Temperatures in the primary shear zone were generally found to vary from ~ 900 to 1300K depending on the cutting speed and the interval of time evaluated. This was expected to cause thermal softening of the Ti-6Al-4V alloy as the material strength typically deteriorates rapidly above temperatures of ~ 350 - 400°C, which would explain the observed formation of adiabatic shear bands leading to the serrated chip morphology.

5. CONCLUSIONS

A preliminary 3D finite element model of the orthogonal cutting process was developed and employed to investigate the machining of Ti-6Al-4V titanium alloy at various cutting speeds. The Johnson-Cook constitutive material relationship and Cockroft-Latham damage model were used to describe workpiece viscoplastic flow stress response and chip formation respectively, which were applied in the FE model through the development of a user defined VUMAT subroutine. In contrast to 'black box' FE packages, the option for implementing customised subroutines in ABAQUS allows users to develop alternative material/damage models more appropriate to the operation under investigation. Chip formation was achieved based solely on the 'physics' of the cutting process, without recourse to any unrealistic assumptions or simplified model definitions such as predetermined failure zones and artificial geometrical features. Predicted cutting forces were found to closely match experimentally measured data with a deviation not exceeding 15% and 6% for tangential and thrust components respectively. While serrated/saw-tooth morphology was predicted in all of the simulations in line with the experimental results, premature failure of elements along the primary shear bands was observed in the model leading to discontinuous chips, which necessitates further improvement of the damage model.

6. ACKNOWLEDGEMENTS

The authors are indebted to the Roberto Rocca Education Program (together with its sponsoring companies Tenaris, Ternium and Techint) and the School of Mechanical Engineering, University of Birmingham for providing a research studentship to R.E. Munoz. Thanks also go to Mr. A. Loat for his help with the orthogonal cutting experiments.

7. REFERENCES

[1] A.O. Tay, M.G. Stevenson and G. De Vahl Davis, Using the finite element method to determine temperature distributions in orthogonal machining, *Proc. Inst. Mech. Eng.* Vol. 188 (1974), 627-638.

[2] T. Ozel and E. Zeren, Finite element modeling the influence of edge roundness on the stress and temperature fields induced by high-speed machining, *Int. J. Adv. Manuf. Technol.* Vol. 35(3-4) (2007), 255-267.

[3] D. Umbrello, R. M'Saoubi and J.C. Outeiro, The influence of Johnson-Cook material constants on finite element simulation of machining of AISI 316L steel, *Int. J. Mach. Tools Manuf.* Vol. 47(3-4) (2007), 462-470.

[4] M. Sima and T. Ozel, Modified material constitutive models for serrated chip formation simulations and experimental validation in machining of titanium alloy Ti-6Al-4V, *Int. J. Mach. Tools Manuf.* Vol. 50(11) (2010), 943-960.

[5] T. Ozel, I. Llanos, J. Soriano and P.J. Arrazola, 3D Finite element modeling of chip formation process for machining Inconel 718: Comparison of FE software predictions, *Mach. Sci. Technol.* Vol. 15(1) (2011), 21-46.

[6] R. Boyer, G. Welsch and E.W. Collings (eds), *Material Properties Handbook: Titanium Alloys*, ASM International, USA, (2007).

[7] G.R. Johnson and W.H. Cook, Fracture characteristics of three metals subjected to various strains, strain rates, temperatures and pressures, *Eng. Fract. Mech.* Vol. 21(1) (1985), 31-48.

[8] M. Calamaz, D. Coupard and F. Girot, A new material model for 2D numerical simulation of serrated chip formation when machining titanium alloy Ti-6Al-4V, *Int. J. Mach. Tools Manuf.* Vol. 48(3-4) (2008), 275-288.
[9] Y. Karpat, Temperature dependent flow softening of titanium alloy Ti6Al4V: An investigation using finite element simulation of machining, *J. Mater. Process. Technol.* Vol. 211(4) (2011), 737-749.
[10] E. Ng, Modelling of the cutting process when machining hardened steel with polycrystalline cubic boron nitride (PCBN) tooling, *PhD thesis, University of Birmingham* (2001).
[11] G. Chen, C. Ren, X. Yang, X. Jin and T. Guo, Finite element simulation of high-speed machining of titanium alloy (Ti-6Al-4V) based on ductile failure model, *Int. J. Adv. Manuf. Tech.* Vol. 56(9-12) (2011), 1027-1038.
[12] R. Shivpuri, J. Hua, P. Mittal, A.K. Srivastava and G.D Lahoti, Microstructure-mechanics interactions in modeling chip segmentation during titanium machining, *CIRP Annals – Manuf. Tech.* Vol. 51(1) (2002), 71-74.
[13] M.G. Cockcroft and D.J. Latham, Ductility and the workability of metals, *J. Inst. Met.* Vol. 96 (1968), 33-39.
[14] D. Umbrello, Finite element simulation of conventional and high speed machining of Ti6Al4V alloy, *J. Mater. Process. Technol.* Vol. 196 (1-3) (2008), 79-87.
[15] G.R. Johnson and W.H. Cook, A constitutive model and data for metals subjected to large strains, high strain rates and high temperatures, *Proc. 7th Int. Symp. Ball., The Hague,* 1983, 1-7.
[16] I. Llanos, J.A. Villar, I. Urresti and P.J. Arrazola, Finite element modeling of oblique machining using an arbitrary Lagrangian-Eulerian formulation, *Mach. Sci. Technol.* Vol. 13(3) (2009), 385-406.
[17] W.S. Lee and C.H. Lin, Plastic deformation and fracture behaviour of Ti-6Al-4V alloy loaded with high strain rate under various temperatures. *Mat. Sc. Eng. A.* Vol. 241(1-2) (1998), 48-59.
[18] J. Lorentzon, N. Jarvstrat and B.L. Josefson., Modelling chip formation of alloy 718, *J. Mater. Process. Technol.* Vol. 209(10) (2009), 4645-4653.
[19] P.J. Arrazola and T. Ozel, Investigations on the effects of friction modeling in finite element simulation of machining, *Int. J. Mech. Sci.* Vol. 52(1) (2010), 31-42.
[20] M.G. Cooper, B.B. Mikic and M.M. Yovanovich, Thermal contact conductance, *Int. J. Heat Mass Trans.* Vol. 12 (1969), 279-300.
[21] S.A. Iqbal, P.T. Mativenga and M.A. Sheikh, An investigative study of the interface heat transfer coeeficient for finite element modelling of high-speed machining, *Proc. Inst. Mech. Eng. B.* Vol. 222 (2008), 1405-1416.
[22] S.L. Soo, *3D modelling when high speed end milling Inconel 718 superalloy*, PhD thesis, University of Birmingham, UK (2003).